Numerical and Experimental Study of Uplift Mobilization of Buried Pipelines in Sands

D. J. Robert[1] and N. I. Thusyanthan[2]

Abstract: Offshore oil and gas pipelines are commonly buried in seabed to provide environmental stability, thermal insulation and mechanical protection. These pipelines are frequently subjected to high thermal and pressure loadings that induce pipeline upheaval buckling (UHB). The uplift resistance provided by the cover soil increases with pipeline upward mobilization and reaches its peak at peak mobilization. This peak mobilization is fundamental for safe UHB designs. This paper highlights that the design guidelines underestimate the peak mobilization. The paper presents full-scale uplift results and finite-element parametric studies in which loose and dense cover soils of up to 3 m (soil cover height to diameter ratio up to 15) and pipeline diameters of 114 and 200 mm were investigated. Results from full-scale and finite-element modeling show that the peak pipe mobilization can be much greater than that suggested by current guidelines, and it is a function of the soil cover height to diameter ratio and soil relative density. A new relationship is proposed to predict peak mobilization from the soil cover height to diameter ratio for a given soil state. **DOI: 10.1061/(ASCE)PS.1949-1204.0000179.** *© 2014 American Society of Civil Engineers.*

Author keywords: Offshore pipelines; Upheaval buckling; Finite element modelling; Large scale tests; Mobilisation; Uplift behaviour; Parametric studies; Det Norske Veritas (DNV); Modified Mohr-Coulomb; Nor-Sand.

Introduction

In recent times, there has been a rapid increase in the use of subsea pipelines to transport high-pressure and high-temperature (HPHT) hydrocarbons. Such pipelines are commonly buried in seabed to provide environmental stability, thermal insulation, and mechanical protection. These buried pipelines, normally operating at high temperature and pressure, have a high tendency to expand, while the friction of surrounding soils tends to restrict its expansion (i.e., axially restrained). Such restraints lead to potential upheaval buckling of pipelines, which has to be mitigated by the appropriate backfill material to prevent consequences of pipeline failures.

Offshore pipelines are often buried by ploughing or jet trenching. The ploughing or jet trenching operation cannot create imperfection free (flat) trenches, thus the pipelines will always have imperfections such as shown in Fig. 1. These imperfections act as the triggering points for the upheaval buckling and the solution for any particular pipeline section will depend on the initial imperfection profile (Croll 1997). In order to prevent upheaval buckling at such imperfection, the pipeline has to be buried deep enough such that the soil cover is sufficient in providing adequate uplift resistance. The required upward movement or mobilization of the pipeline to achieve the desired uplift resistance is a vital design parameter, in that pipeline integrity under operating conditions relies on its value (Thusyanthan et al. 2010, 2011).

There are several analytical models developed in literature to address the upheaval resistance from backfill soil (Pedersen and Jensen 1988; Schaminee et al. 1990; Palmer et al. 1990), but all assume that the peak resistance is developed when the pipe is displaced some predefined mobilizations. Peak uplift resistance can be obtained from Eq. (1) as per Det Norske Veritas (DNV) RP F110 (DNV 2007)

$$\frac{R_{\text{peak}}}{\gamma' HD} = 1 + \left(0.5 - \frac{\pi}{8}\right)\frac{D}{H} + f_p\left[\frac{1}{\gamma' HD} \times \left(H + \frac{D}{2}\right)^2\right] \quad (1)$$

DNV provides peak mobilization, δ_f, as $0.005H$ to $0.008H$, where H is the soil cover to top of the pipeline. Table 1 summarizes the DNV RP F110 (DNV 2007) guidelines on mobilization and peak uplift factor for sand and rock. ASCE (1984) defines that the peak resistance in granular backfill is achieved once the pipe mobilizes (δ_f) to 0.01–0.015 $(H + D/2)$. Hence it is clear that the δ_f defined in standards have not captured any effects arising from D or soil density. Results from the full-scale experiments (Thusyanthan et al. 2010) reveal that the mobilization displacements can be significantly higher than the current guidelines for pipes having higher H or H/D ratios. Thusyanthan et al. (2010) has shown, using a design example, the importance of using the correct peak mobilization in upheaval buckling (UHB) design of HPHT pipelines. Underestimation of peak mobilization can lead to nonconservative UHB designs. Wang et al. (2012) present experimental data from shallowly buried pipelines to show that the δ_f/H ranges from 1 to 8% for $H < 0.6$ m. If a HPHT needs to be further mobilized than assumed in the original design to achieve the required backfill resistance, it can lead to pipeline overstressing and potentially lead to failure. In addition, if the mobilization is limited due to pipeline stress limits, the peak uplift resistance cannot be fully utilized in upheaval buckling design as shown in Fig. 2. Therefore, the correct mobilization curve is critical for safe and economical design of HPHT pipelines and hence the correct prediction of peak mobilization is an important factor in pipeline design. This paper presents finite-element (FE) modeling and experimental results of pipeline's upward full mobilization required to obtain the peak uplift resistance of buried pipelines in granular medium. Full-scale experimental results were compared with the FE results for validation,

[1]Lecturer in Civil Engineering, School of Civil, Environmental and Chemical Engineering, RMIT Univ., Melbourne 3001, Australia (corresponding author). E-mail: dilan.robert@rmit.edu.au

[2]Principal Geotechnical Engineer, Consulting Services Dept., Saudi Aramco, Dhahran 31311, Saudi Arabia. E-mail: it206@cantab.net

Note. This manuscript was submitted on September 10, 2013; approved on May 27, 2014; published online on July 21, 2014. Discussion period open until December 21, 2014; separate discussions must be submitted for individual papers. This paper is part of the ***Journal of Pipeline Systems Engineering and Practice***, © ASCE, ISSN 1949-1190/04014009 (10)/$25.00.

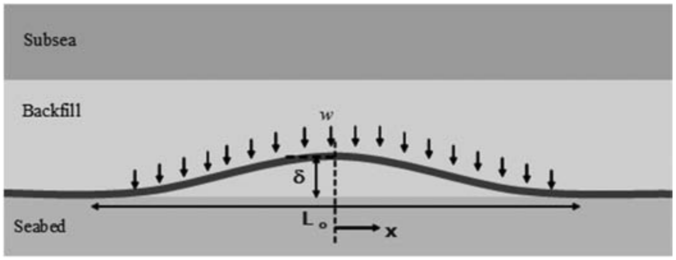

Fig. 1. Typical upheaval buckling profile of a buried offshore pipeline

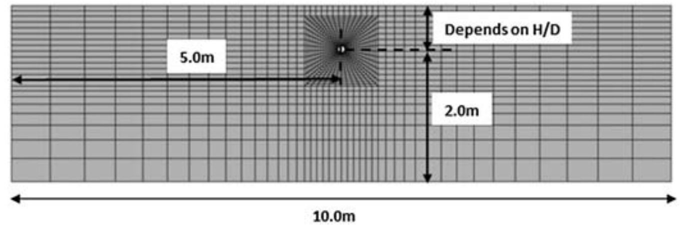

Fig. 3. Geometry and mesh discretization of the model used for the FE analyses

Table 1. Recommended Values from DNV-RP-F110 (DNV 2007)

Backfill soil type	Mobilization distance δ_f	Pedersen uplift factor f_p	DNV limitation
Loose SAND	0.5–0.8%H	0.1–0.3	$3.5 \leq H/D \leq 7.5$
Medium or dense SAND	0.5–0.8%H	0.4–0.6	$2 \leq H/D \leq 8$
Rock	20–30 mm	0.5–0.8	$2 \leq H/D \leq 8$, particle size (25–75 mm)

Note: δ_f is given as 0.005–0.01H in the text of DNV RP F110 (DNV 2007, p. 44).

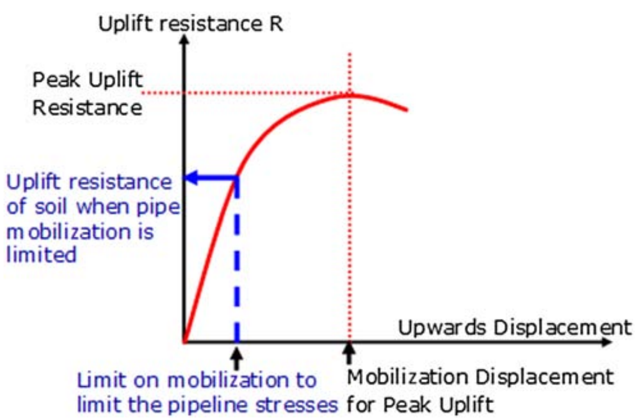

Fig. 2. Typical uplift resistance versus pipeline mobilization curve

and parametric study with varying D, soil relative density, and H/D ratios were undertaken to understand the influence of these factors on peak mobilization.

FE Modeling of Uplift Mobilization in Buried Pipelines

Overview

FE modeling of uplift mobilization was undertaken in *ABAQUS* with geometric nonlinearity and large strain formulation. This ensures that the large strains induced in the elements around the pipe during uplift of the pipe are modeled correctly. The nonlinear geometry option (NLGEOM) in *ABAQUS* considers the changes in geometry during the analysis, and thus the equilibrium is achieved using the current configuration (i.e., current nodal position) of the model. All the analyses were performed under plane strain conditions and the model uses soil and pipe elements with eight-noded biquadratic, plane strain, reduced integration (CPE8R) elements (*ABAQUS*). Fig. 3 shows the geometry and the mesh discretization of the FE model used to simulate the vertically loaded pipeline experiments. The wall boundaries were assumed to be smooth and supported only in the normal direction. The pipe was pulled vertically by imposing equal uplift displacement on all pipe nodes and was set to move freely in the lateral direction. Adaptive meshing has been incorporated in the analyses to control the mesh distortions that result from large deformations of the soil caused by upward pipe displacements. The behavior of the pipe is assumed to be linear elastic, whereas nonlinear elasticity is assumed for the behavior of soil surrounding the pipe.

The interaction between the pipe and soil has been modeled on the basis of the coulomb friction model, which relates the maximum allowable frictional shear stress (τ_{crit}) across the interface to the contact pressure (σ_n') between the pipe and soil. The allowable frictional stress is given by $\mu\sigma_n'$, where μ (tan ϕ_μ) is the interface friction coefficient. The contacting surfaces will stick together and the behavior remains elastic when $\tau < \tau_{\text{crit}}$. The slipping along the interface between the buried pipe and surrounding soil takes place once τ produced in the interface reaches τ_{crit}. This behavior was modelled using the finite movement solution available in *ABAQUS*. In the current study, ϕ_μ was set to equal to half of the peak frictional angle of soil (Cheong 2006; Yimsiri et al. 2004).

FE modeling and assessments were undertaken in three phases: studies 1, 2, and 3. In Study 1, results of full-scale experiments were simulated by FE analyses to understand the underlying mechanisms of soil-pipeline interaction in upward pipe movements. The second and third studies were parametric studies conducted to investigate the effect of initial soil states (loose and dense), pipe embedded depths, and pipe diameters on the peak mobilizations during uplift of a pipeline. Table 2 summarizes the FE studies performed under various conditions.

Study 2 involved FE analyses of uplift pipe movements under two different initial sand states (i.e., loose state and dense state). Study 3 was performed to investigate the effect of pipe diameter on peak mobilizations when behaving in the field sand. Particle size distribution of sands whose properties were used in studies 1, 2, and 3 are shown in Fig. 4.

Constitutive Models

Pipe Model

The pipe was assumed to have a Young's modulus, E_p, of 204 GPa with a Poisson's ratio, υ_p, of 0.3 for all the analyses conducted in this paper. Nevertheless, because the pipe was displaced as a rigid body, the pipe stiffness is essentially infinity, and thus the soil stresses imposed on the pipe and the pipe deformations are negligible (Cheong 2006).

Table 2. Summary of Uplift FE Analyses Performed

FE study	Aim of the study	Soil constitutive model	Pipeline diameter (m)	H/D
Study 1	To model full-scale experiments To study effect of different soil model To study effect of H/D	Nor-SAND and modified Mohr-Coulomb	0.2	2, 6, 8, 12.5
Study 2	To study effect of soil relative density To study effect of H/D	Modified Mohr-Coulomb	0.2 0.114	2, 6, 8, 12.5, 15 0.5, 3.5, 8, 11, 15
Study 3	To study effect of pipeline diameter To study effect of H/D	Modified Mohr-Coulomb	0.2 0.114	2, 6, 8, 12.5, 15 0.5, 3.5, 8, 11, 15

Soil Constitutive Models

Soil behavior was modeled using the modified Mohr-Coulomb (MMC) constitutive model. The model was chosen considering its simplicity, easiness to use, CPU time, and higher community understanding of the model, i.e., simplicity refers a relatively simple model compared to advanced constitutive models such as Nor-Sand (NS) and Cam-Clay. Also, the Mohr-Coulomb model only demands a few parameters that can be easily determined through direct shear tests, unlike other models that demand their parameters through proper controlled triaxial testing. Further, the Mohr-Coulomb model is widely popular in the community for modeling the behavior of soils due to its relative simplicity and the need of popular soil properties (such as friction and dilation of soils). The modified Mohr-Coulomb model is a modified version of Mohr-Coulomb introduced to capture the strain softening behavior of the material (Robert and Soga 2010). The softening behavior has been captured by reducing the mobilized friction (ϕ'_{mob}) and dilation angle (ψ_{mob}) with an increase in plastic deviatoric shear strains (γ^p_{dev}). The elastic behavior of the model remains as defined in the original Mohr-Coulomb model and the plastic behavior depends on the softening of the yield surface and flow potential based on deviatoric strains.

In this study, the variations of ϕ'_{mob} and ψ_{mob} as given by Eqs. (2) and (3) have been incorporated into *ABAQUS/STANDARD* through a user subroutine called USDFLD written in FORTRAN. Here, the $\phi_{\max}$ and ϕ_{crit} are the peak and critical state friction angles, respectively, and $\psi_{\max}$ and ψ_{res} are the ultimate and residual dilation angles, respectively. The plastic deviatoric shear strain at softening completion is noted by γ^p_f. The calibration and validation of the model based on triaxial compression data as well as mesh sensitivity effects can be found in Robert (2010).

$$\phi'_{\text{mob}} = \phi'_{\max} - \left(\frac{\phi'_{\max} - \phi'_{\text{crit}}}{\gamma^p_f}\right) \cdot \gamma^p_{\text{dev}} \quad \text{for } 0 \leq \gamma^p_{\text{dev}} \leq \gamma^p_f = \phi_{\text{crit}} \quad \text{for } \gamma^p_{\text{dev}} > \gamma^p_f \tag{2}$$

$$\psi_{\text{mob}} = \psi_{\max}\left(1 - \frac{\gamma^p_{\text{dev}}}{\gamma^p_f}\right) \quad \text{for } 0 \leq \gamma^p_{\text{dev}} \leq \gamma^p_f = \psi_{\text{res}} \quad \text{for } \gamma^p_{\text{dev}} > \gamma^p_f \tag{3}$$

For Study 1, the NS model was also used because the model requires single set of input parameters for a particular sand type irrespective of its initial state. The Nor-Sand model is a generalized Cambridge-type constitutive model for sand developed on the basis of the critical state theory. It uses the state parameter concept (Been and Jefferies 1985) and attempts to accurately reproduce dilation and softening on the dry side of the critical state. This is achieved by postulating infinite isotropic normal consolidation loci (NCLs), which allows a separation of the intrinsic state from the overconsolidation state. A main feature of the Nor-Sand model is the use of rate-based hardening using the state parameter, ξ, to size the yield surface. The original Nor-Sand model was proposed by Jefferies (1993) and was implemented into implicit finite elements by Dasari and Soga (2000). In order to enhance the model performance, three modifications were made by Cheong (2006). They include (1) a new definition for the critical state, (2) lode angle dependency on the critical state parameter, and (3) the evolution of yield surface with respect to plastic shear strain. In the current study, Nor-Sand code was implemented into explicit finite elements in order to be benefited by explicit simulations (Robert 2010).

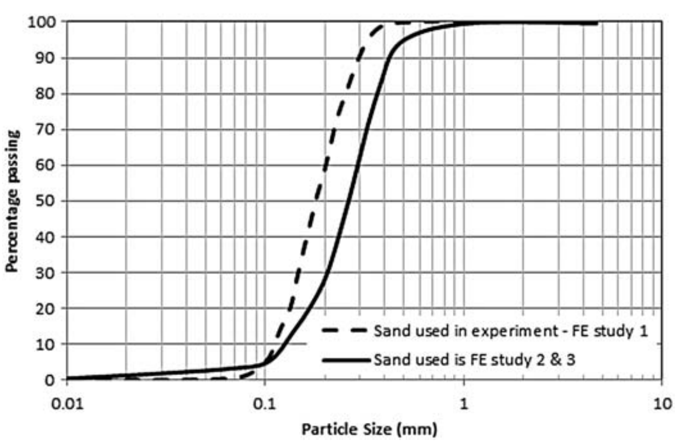

Fig. 4. Particle size distribution of sands whose properties were used in FE analysis

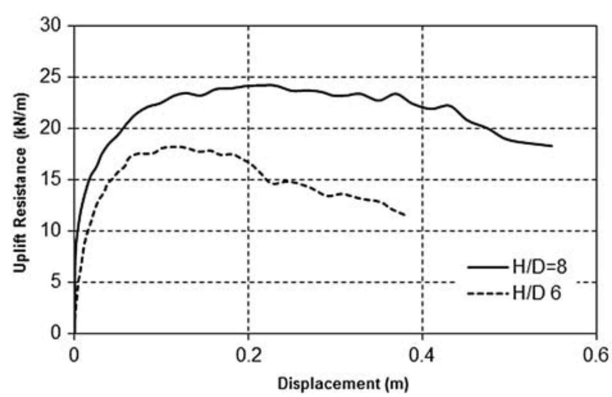

Fig. 5. Results of the full-scale uplift test in sand, pipeline diameter $D = 200$ mm

Table 3. Peak Mobilization Distance Predicted by DNV and ASCE versus Measured from Full-Scale Experiment Results

H (mm)	Peak mobilization DNV 0.5%H to 0.8%H (mm)	Peak mobilization ASCE $0.01(H+D/2)$ to $0.015(H+D/2)$ (mm)	Peak mobilization measured in full-scale experiment (mm)	Peak uplift factor f_p from full-scale experiment
1,200	6 to 9.6	13 to 19.5	110	0.56
1,600	8 to 12.8	17 to 15.5	215	0.43

Note: $D = 200$ mm.

Overview of the Full-Scale Experiments

Full-scale uplift experimental results are used to understand the mobilization required to obtain the peak uplift resistance in buried pipeline. Full-scale experiments were carried out using a steel pipeline of 3 m in length and 200 mm in diameter. A full-scale test tank of 2,250 mm width, 2,500 mm height, and 5,000 mm length was used in the experiment. The backfill cover was loose fine sand (similar to Fraction E sand) with bulk unit weight of 15 kN/m^3. A series of uplift experiments were carried out at various cover heights. In this paper, results of only H/D ratios of 6 and 8 are presented in Fig. 5 for comparison with FE modelling. The peak uplift resistances for H/D ratios 6 and 8 tests are obtained at a mobilization of 110 and 215 mm, respectively.

Table 3 summarizes the peak mobilization measured from these full-scale tests against peak mobilization prediction based on DNV and ASCE guidelines. It can be seen that the measured peak mobilization displacements are significantly higher than those predicted by DNV and ASCE guidelines. One of the reasons for these guidelines to underpredict the peak mobilization for cover heights of 1.2 and 1.6 m is that these guidelines were based on results from laboratory tests that used predominantly shallower cover heights, possibly with cover heights less than 0.5 m. Thus, peak mobilization based on current DNV or ASCE guidelines could lead to nonconservative designs for deeper covers.

Table 4. Soil Constitutive Model Parameters Used in FE Analyses of Study 1

Constitutive model	Parameters	Value
Nor-Sand	Shear modulus constant (A)	150
	Pressure exponent (n)	0.5
	Poisson's ratio (ν)	0.2
	Critical state ratio (M)	1.33
	Maximum void ratio ($e_{\max}$)	1.014
	Minimum void ratio ($e_{\min}$)	0.613
	N value in flow rule	0.33
	Hardening parameter (h)	20
	Maximum dilatancy coefficient (χ)	2.5
	Switch to use constant or exp H	0.0 (exp)
	Tolerance (TOL)	0.001
Modified Mohr-Coulomb	Peak friction angle $\phi'_{\max}$ (°)	35°
	Peak dilation angle $\psi_{\max}$ (°)	1.25°
	Critical state friction angle ϕ_{crit} (°)	33°
	Plastic deviatoric shear strain at softening completion γ_f^p	0.3
	E (kPa)	500
	ν	0.3
	c' (kPa)	0.5
	I_r at pipe level	0.1

Note: Input parameters for constitutive models were calibrated on the basis of Grade E sand.

FE Results

Study 1: Numerical Modeling of Full-Scale Uplift Experiment

Full-scale experiments were numerically simulated to investigate the capability of the developed numerical models to predict the experimental pipe uplift behavior. The input parameters for the Nor-Sand model and modified Mohr-Coulomb model, which were based on Grade E sand, are summarized in Table 4.

Experimental results from $H/D = 6$ was used to calibrate the FE model. Fig. 6(a) shows the results from both the FE analyses and full-scale experiment. Using the same calibrated properties, the FE analysis was then performed to predict the uplift resistance versus mobilization behavior for burial of $H/D = 8$. Fig. 6(b) shows the results from both the FE analyses and full-scale experiment for $H/D = 8$.

The peak load prediction from both the constitutive models matches reasonably well with the experimental data for the

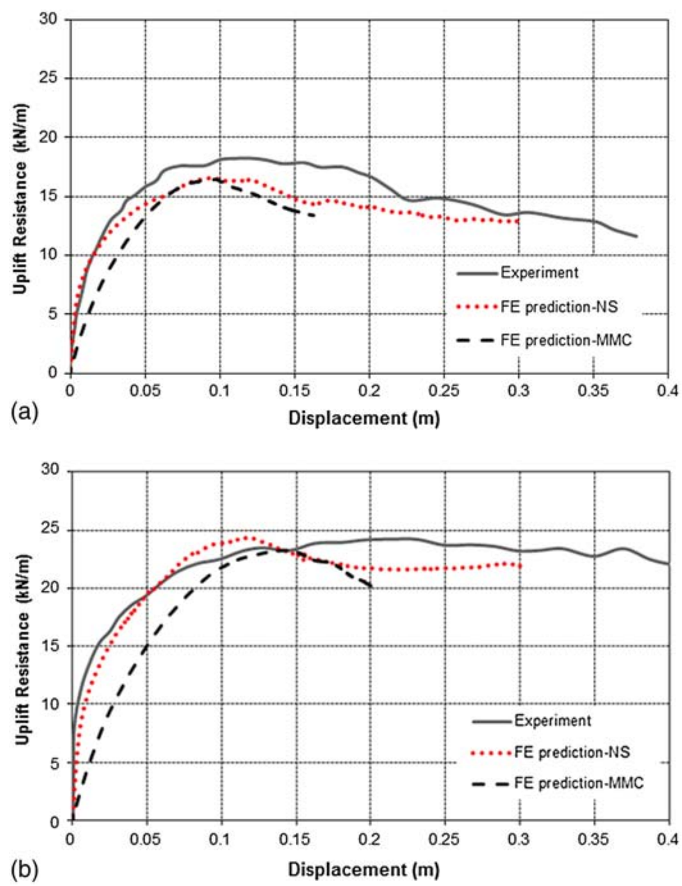

Fig. 6. FE uplift results compared with the full-scale uplift experimental results: (a) $H/D = 6$; (b) $H/D = 8$

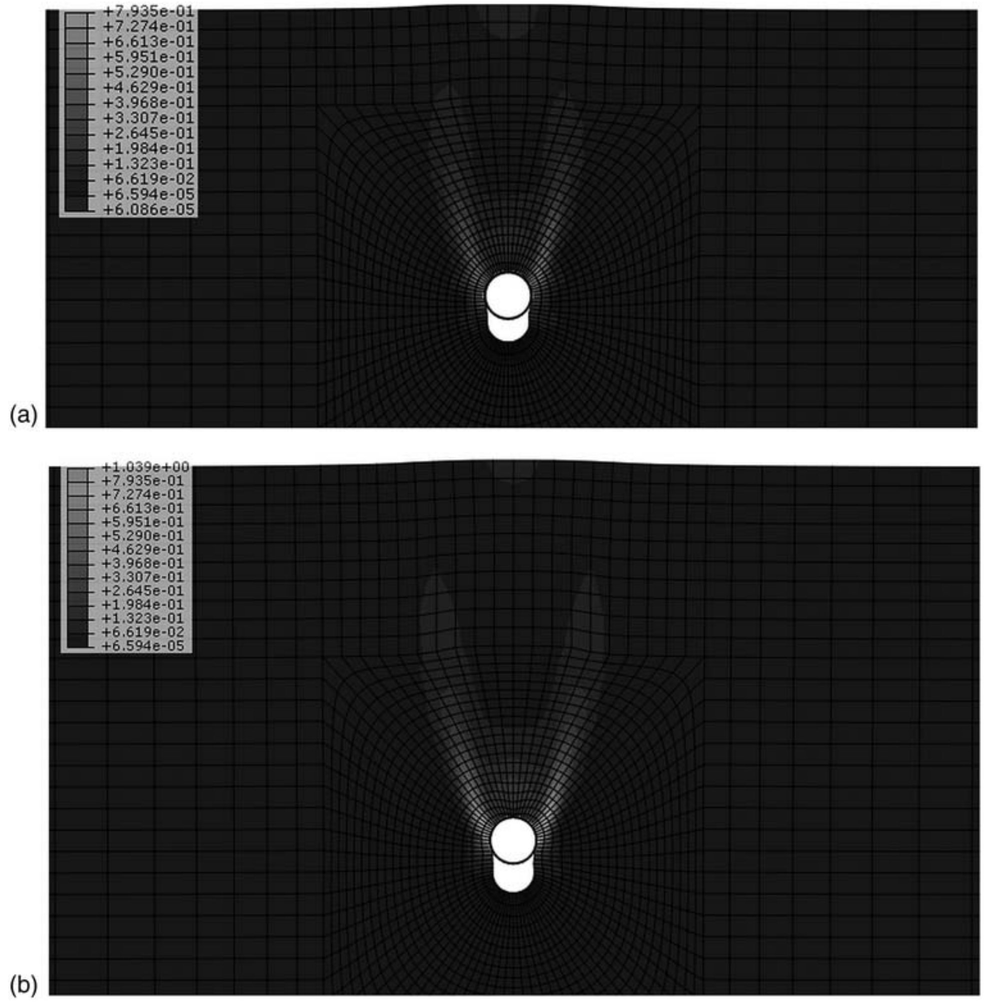

Fig. 7. FE model prediction of full-scale experiments, shear strain plot at peak uplift resistance: (a) $H/D = 6$; (b) $H/D = 8$

$H/D = 8$ case. The FE predictions of peak mobilization for $H/D = 8$ is lower than the peak mobilization observed from experiment. However, the experiment curve is relatively flat at the peak uplift resistance, thus peak mobilization from FE is acceptable. The initial stiffness response from the Nor-Sand model has a better match to the experimental data than that from modified Mohr-Coulomb model due to the use of state parameter based hardening approach in Nor-Sand. The deformation mechanism from FE analyses plotted in terms of shear strain contours is shown in Fig. 7.

Further parametric FE study was undertaken to investigate the effect of H/D on peak mobilization. The parametric study was undertaken using the MMC soil model with properties given in Table 5. Fig. 8 shows the force-displacement response obtained from these analyses. It can be seen from the results that the pipes buried at deeper depths attain peak mobilizations at slower rates

Table 5. Parameters Used for the Modified Mohr-Coulomb Model Used in Studies 2 and 3 (Data from Robert 2010)

H/D	γ_d (g/cm^3)	I_r at pipe level	E (kPa)	ν	c'(kPa)	$\phi'_{\max}$ (degrees)	$\psi_{\max}$ (degrees)	ϕ_{crit} (degrees)	γ_f^p
2.0	1.402	0.1	1,000	0.3	0.5	34	1.25	33.0	0.3
2.0	1.60	4.5	3,000	0.3	0.5	45	15.0	33.0	0.3
6.0	1.409	0.1	1,000	0.3	0.5	34	1.25	33.0	0.3
6.0	1.658	4.5	3,000	0.3	0.5	45	15.0	33.0	0.3
8.0	1.411	0.1	1,000	0.3	0.5	34	1.25	33.0	0.3
8.0	1.675	4.5	3,000	0.3	0.5	45	15.0	33.0	0.3
12.5	1.415	0.1	1,000	0.3	0.5	34	1.25	33.0	0.3
12.5	1.703	4.5	3,000	0.3	0.5	45	15.0	33.0	0.3
15.0	1.417	0.1	1,000	0.3	0.5	34	1.25	33.0	0.3
15.0	1.717	4.5	3,000	0.3	0.5	45	15.0	33.0	0.3

Note: Input parameters were determined using element tests.

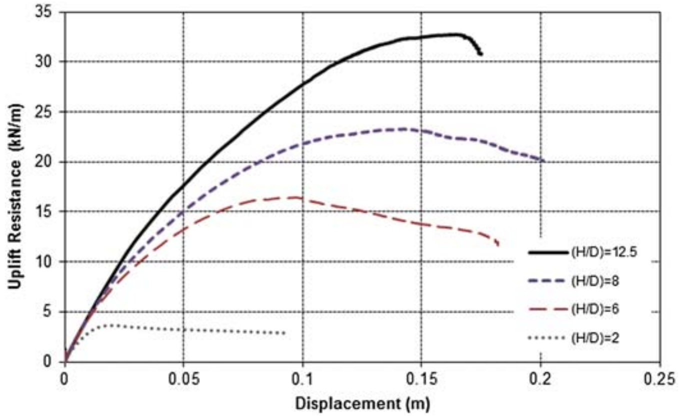

Fig. 8. Results of the parametric study 1, $D = 200$ mm, uplift resistance versus uplift displacement

due to the enhanced soil strengths generated by higher confining stresses. In addition, load-displacement plots show the capability in generating strain softening behavior of post-peak response using the modified Mohr-Coulomb model.

The first parametric study was conducted to investigate the mobilization effect of the pipe used in full-scale tests under varying H/D conditions on the basis of the same sand. The plot between the normalized displacement against embedment ratio in Fig. 9 shows that the peak dimensionless mobilizations predicted from large-scale tests as well as from FE analyses are significantly higher than that suggested by DNV guidelines [DNV RP F110 (DNV 2007)]. This reveals that the current standards are not capable of capturing the correct peak mobilization (i.e., underestimating) for upheaval buckling of pipelines. The peak mobilizations can be normalized either by the embedment depth or by pipe diameter. Owing to the potential for localized failure mechanism criteria, the pipe diameter (a local length scale) can be a more appropriate mechanism (Williams et al. 2013) for normalization of the peak mobilizations. This normalization has been adopted for the remainder of this paper.

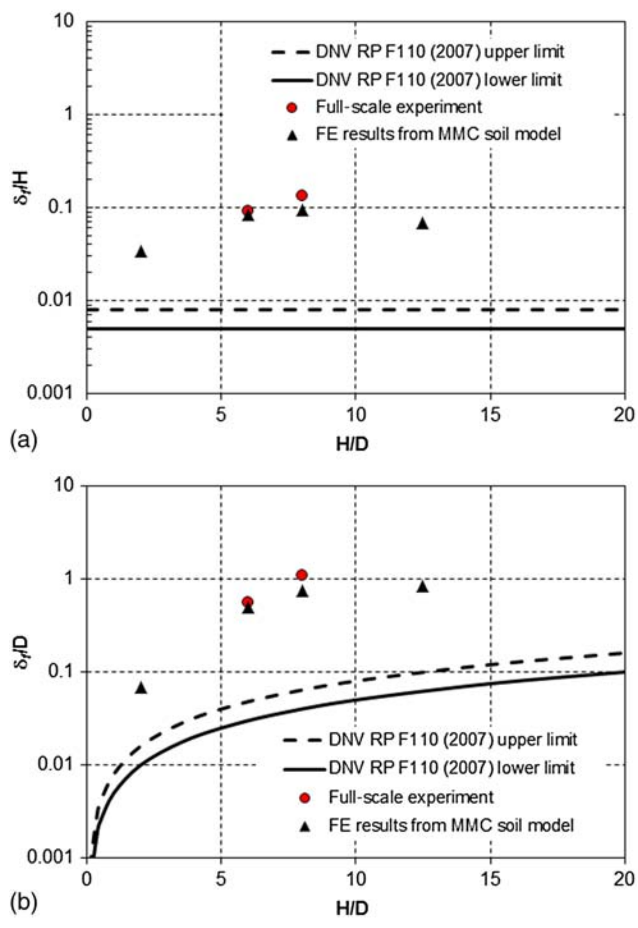

Fig. 9. Summary of the results of the parametric study 1: (a) peak mobilization normalized by H; (b) peak mobilization normalized by D

Study 2: Effect of Relative Density of Backfill Soil on Peak Mobilization Distance

Effect of relative density of peak mobilization was investigated in Study 2. Bolton's (Bolton 1986) relative dilatancy index, I_r, can be related to relative density, I_d, using Eq. (4) as defined in Bolton (1986), where p' is the mean effective confining stress at the pipeline level.

$$I_r = I_d(10 - \ln p') - 1 \tag{4}$$

FE analyses for pipeline uplift behavior were performed under two different initial sand states, pertaining to I_r of 0.1 and 4.5 for loose and dense states of sands, respectively. These represent relative densities of 13–18% and 65–90% for I_r of 0.1 and 4.5, respectively. The MMC soil model with model parameters, which were based on triaxial tests performed by Robert (2010), as shown in Table 5 were used in the study.

The uplift resistance versus upward mobilization results from FE analyses are presented in Figs. 10 and 11 for loose and dense sands, respectively. It can be seen from the figures that the pipes in denser sands attain peak mobilizations faster. Load-displacement plots also show the capability in generating strain softening behavior of post-peak response using the modified Mohr-Coulomb model. A clearer softening band has resulted at the post-peak response of the pipes behaving in denser sands. Fig. 12 summarizes the results of peak mobilization normalized by pipe diameter D. As H/D increases, the difference in peak mobilization of loose and dense soil states also increases, and at H/D ratios of 10–15, the difference in δ_f/D is more than double compared with the difference at smaller H/D ratios (i.e., $H/D < 5$). It can also be seen from

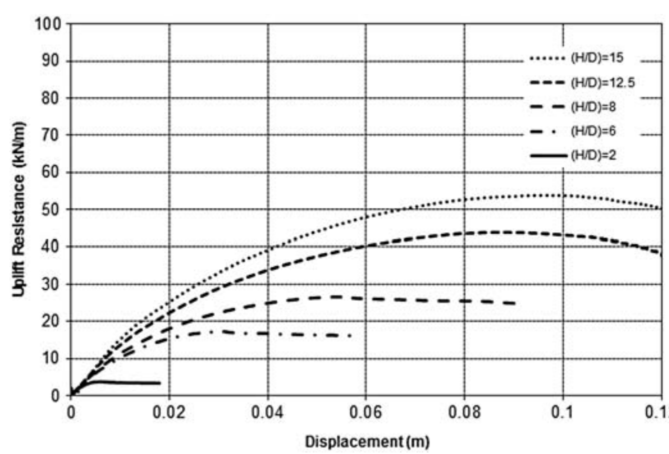

Fig. 10. Uplift resistance versus displacement results from loose sand, $D = 200$ mm

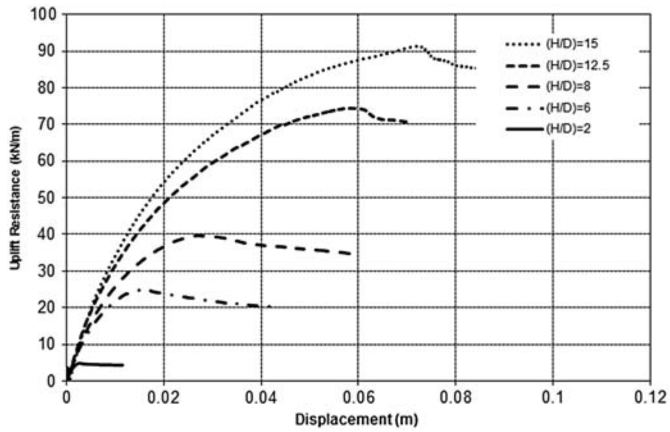

Fig. 11. Uplift resistance versus displacement results from dense sand, $D = 200$ mm

the results that peak mobilizations for loose to dense state of the sands are within the DNV and ASCE estimates at shallower embedded depth (for $H/D = 2$), whereas the DNV guideline underestimates the peak mobilization when the pipe burial gets deeper (i.e., $H/D > 5$). The ASCE guideline also underestimates the peak mobilization at higher H/D ratios. At shallower pipe embedded depths ($H < 0.5$ m), soil fails mainly by global shearing mechanism. In such depths, the soil dilatancy is more dominant and hence the shear bands are well defined, causing it to yield smaller peak mobilizations. However, at deeper burial depths soil fails mainly due to local shear failures induced by high overburden stresses, i.e., by deep failure mechanism (Trautmann and O'Rourke 1983). This result generates extended mobilizations as can be depicted from experimental data as well as from numerical predictions.

Study 3: Effect of Pipeline Size on Peak Mobilization

Parametric FE assessments were carried out to understand the effect of pipeline size on peak mobilization. Uplift FE analyses on pipelines with diameters of 200 and 114 mm were performed in both loose and dense soil states. The MMC soil model with similar properties as in Study 2 was used for this study.

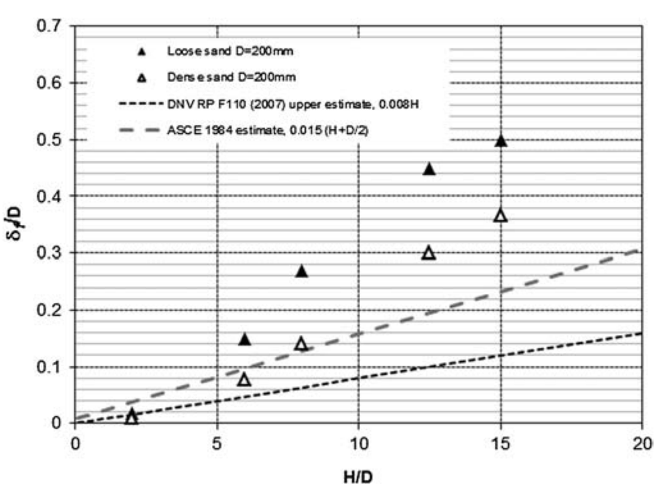

Fig. 12. Summary of Study 2 results, dimensionless mobilization versus H/D ($D = 200$ mm)

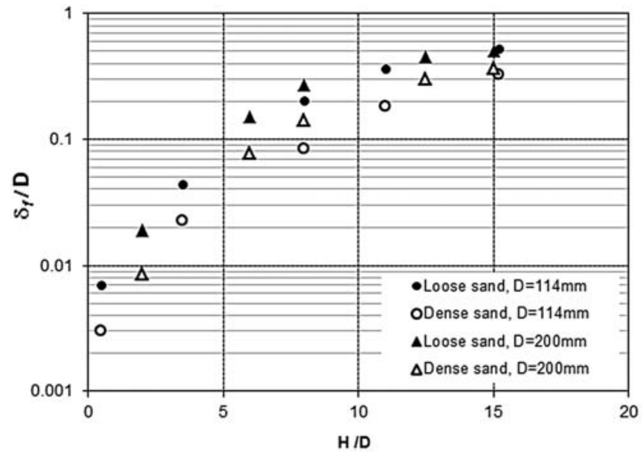

Fig. 13. Summary of Study 3 results, normalized peak mobilization versus H/D

The results of these analyses are shown in Fig. 13 for both $D = 200$ mm and $D = 114$ mm. The results are presented in terms of normalized peak mobilizations and embedment depths. It can be seen that the normalized mobilizations are hardly affected by the pipeline size at varied embedment depths. Also, it is evident that the relative density of soil has a bigger influence on the peak mobilization than the pipeline size.

Discussion

A summary of the results from parametric studies 1 and 2 are presented in Fig. 14. The peak mobilization is normalized by D in the figure. It is evident from the results that for given soil properties, the δ_f/D increases in log scale with H/D until approximately $H/D = 8$. It can also be concluded that for a given soil type, the relative density greatly affects the peak mobilization distance at all H/D ratios. For $H/D > 6$, the δ_f/D seems to be between 10 and 100%. It is also evident that the DNV (2007) guideline on peak mobilization is a great underestimation. This underestimation in the guideline can be mainly attributed to the fact that these guidelines were based on uplift tests under laboratory conditions in

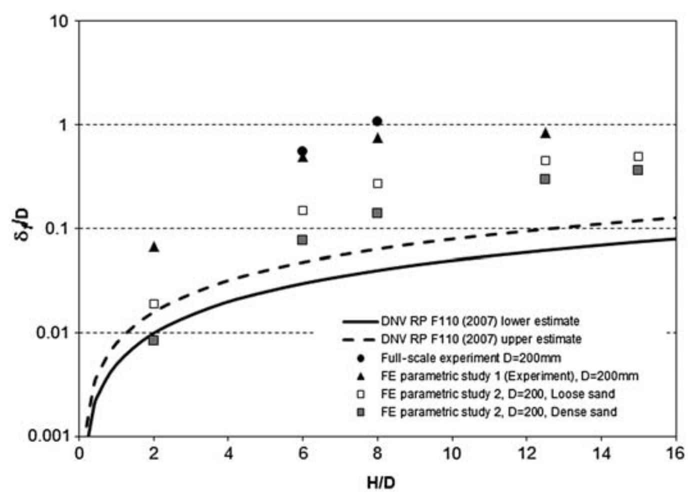

Fig. 14. Peak mobilization normalized by D; summary of parametric studies 1 and 2

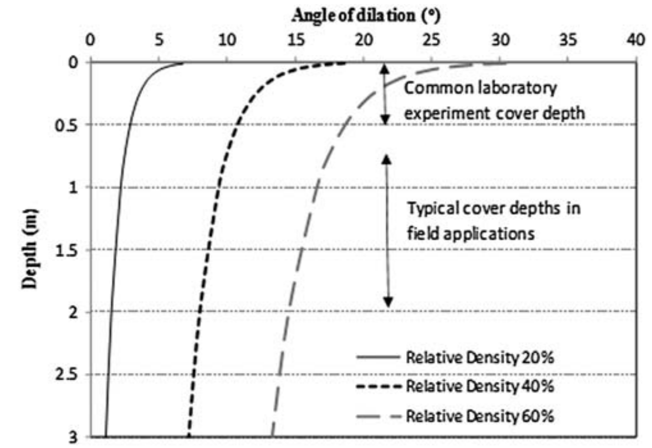

Fig. 15. Angle of dilation versus depth for sands with the relative densities of 20, 40, and 60%

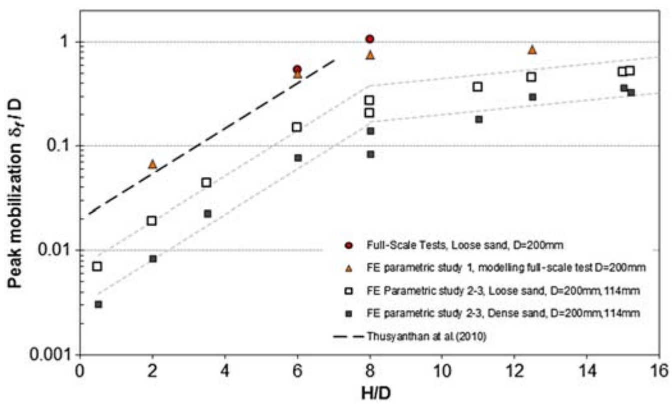

Fig. 16. Peak mobilization normalized by D; summary of parametric studies 1, 2, and 3

which the cover soil investigated is typically less than 0.5 m for practical reasons. This in turn results in peak uplift resistance being reached at small mobilizations due to high soil dilatancy contribution, which is more prominent at these lower stress levels. This can be demonstrated by viewing the angle of dilation versus depth for sands. The angle of dilation under plane strain conditions can be assessed using Bolton's formulation (Bolton 1986) and has been shown in Fig. 15. It is clear from the figure that under typical laboratory experiments in which the cover height is likely to be less than 0.5 m, the dilation angle is much higher than at typical field cover heights. This is one of the key reasons for laboratory experiments to measure peak uplift at small mobilizations. Furthermore, the burial depths of oil and gas pipelines in the field are much greater than 0.5 m. For onshore pipelines, ASME B31.8 (ASME 2012) provides minimum cover depth to be 0.6 to 0.9 m depending on the location, and similarly PD8010-1 (British Standards 2004) states the minimum cover as 0.9 m. For offshore pipelines, it is often in the range of 1.5–2.5 m, where the minimum burial depth is mostly determined by protection and mitigation for upheaval buckling requirements. Thus, most of the published pipeline uplift experimental results, which are mainly based on shallow cover depths (Williams et al. 2013), are not directly applicable for field application and the results of such experiments should not be extrapolated.

Fig. 16 presents the peak mobilization results normalized by D obtained from all the studies conducted (1, 2, and 3). The figure also shown the peak mobilization equation proposed by Thusyanthan et al. (2010), which is Eq. (5) with A as 0.2 and B as 0.5. It is evident from the parametric study results shown in Fig. 16, that for a given soil state and conditions, peak mobilization normalized with D seems to have a linear increase in log scale with H/D until approximately H/D of 8. Beyond $H/D = 8$, the increase still exists but at a much slower rate. The transition at approximately $H/D = 8$ is observable from the results. Hence, it is reasonable to suggest that a fundamental change in the pipeline uplift mechanism may be occurring when H/D ratios reach 8, thus leading to a change in the relationship between peak mobilization and H/D ratio. Further research at this H/D ratio is required to

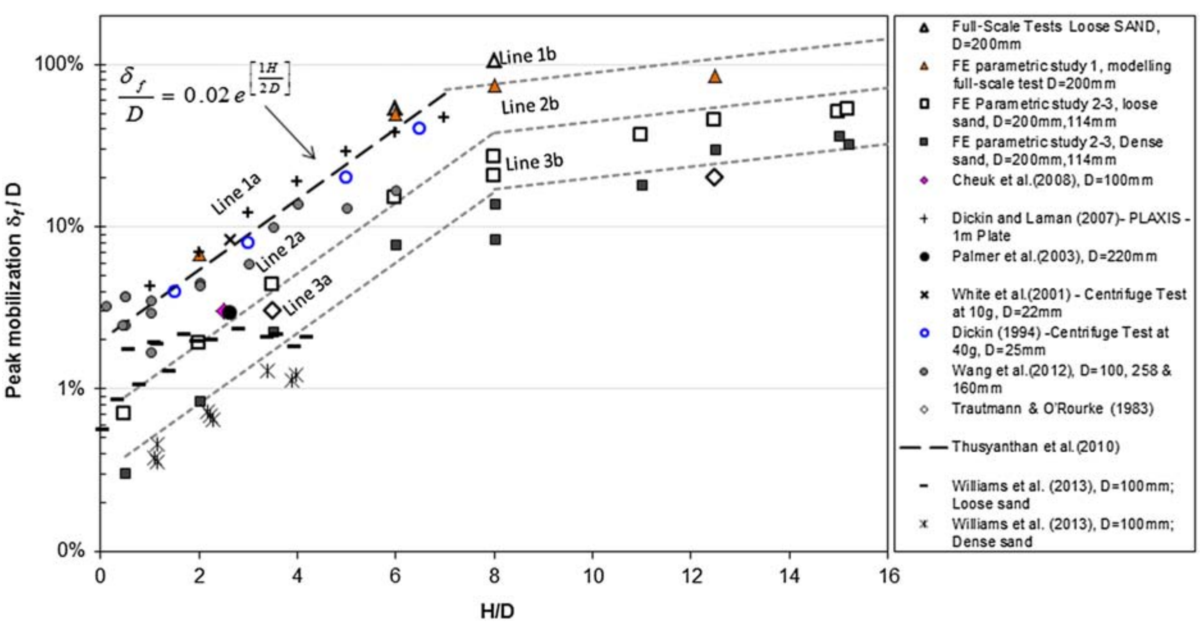

Fig. 17. Peak mobilization (δ_f) normalized by D versus H/D; summary of FE parametric studies results and published data from literature

Table 6. Peak Mobilization Prediction Line Parameters

Line	Value of A	Value of B
1a	0.200	0.50
2a	0.007	0.50
3a	0.003	0.50
1b	0.400	0.08
2b	0.017	0.08
3b	0.070	0.08

fully understand the various factors affecting the pipeline behavior in this condition.

Fig. 17 summarizes all the results from current parametric studies together with peak mobilization data from various literature. The trend lines for the peak mobilization are also shown as lines 1a, 1b, 2a, 2b, 3a, 3b. The trend lines are given by Eq. (5) with A and B values are presented in Table 6. The peak mobilization line proposed by Thusyanthan et al. (2010) seems to provide an upper bound estimate for the peak mobilizations from numerical and experimental results from current research and also from past published data up to $H/D = 8$

$$\frac{\delta_f}{H} = Ae^{[B(H/D)]} \tag{5}$$

Conclusion

Upheaval buckling is a common design issue encountered for buried pipelines that operate at high temperatures and pressures. Peak mobilization is a critical design parameter for safe and economical upheaval buckling design. The current guidelines (DNV, ASCE) provide peak mobilization as a function of backfill cover alone. For instance, DNV RP F110 (DNV 2007) defines the peak mobilization as 0.005–0.01H, stating that δ_f seems to be independent of H/D ratio. ASCE (1984) defines that the peak resistance in granular backfill is achieved once the pipe mobilizes to 0.01–0.015 of soil cover to the center of the pipeline.

Based on both numerical and full-scale experimental results, this paper concludes that the mobilization required to obtain the peak uplift resistance in buried pipelines in sands depends on H/D ratio, H, and relative density of the backfill sands. A series of parametric studies were conducted to investigate the effect of H/D, relative soil density, and pipeline diameter on peak mobilization. Peak mobilization under H/D ratios up to 15 (H up to 3 m) under loose and dense soil covers were numerically investigated with two pipeline diameters (114 and 200 mm). Results of FE parametric studies and full-scale experiments show that the peak mobilization displacements can be significantly higher than suggested by DNV (2007) and ASCE (1984) guidelines, especially when cover depths are greater than 0.5 m. This is attributed to the fact that the guidelines are mainly based on published results from laboratory experiments where the soil cover often was less than 0.5 m, and at these low stress levels, soil dilation (Fig. 15) dominates the mobilization behavior, leading to smaller peak mobilization. However, the burial depths in field application is often greater than 0.9 m where soil dilation plays a smaller role than at shallower depths, thus peak mobilization is much greater than current guideline predictions.

Fig. 17 presents peak mobilization trend lines that can be used to estimate peak mobilization for a given soil state at various H/D ratios. The trend line changes at approximately $H/D = 8$, and this could be attributed to the soil failure mechanism changing from global to flow-around mechanism. The dimensionless chart presented in this paper is a starting point for initial UHB assessment in front end engineering designs (FEED). Other factors, such as saturation ratio, particle size distribution, and bulk density, were not investigated in this paper but are also likely to affect the peak mobilization distance.

Notation

The following symbols are used in this paper:

- D = pipe external diameter (L);
- E_p = Young's modulus of pipe ($ML^{-1}T^{-2}$);
- f = simplified uplift factor (–);
- f_p = peak uplift factor at peak uplift resistance [consistent with DNV-RP-F110 (DNV 2007)] (–);
- H = depth of soil cover measured from soil surface to pipe crown (L);
- I_d = relative density of soil (–);
- I_r = relative dilatancy index of soil (–);
- p' = mean effective stress at the pipeline level ($ML^{-1}T^{-2}$);
- R = net soil downward resistance to UHB per unit pipe length (MT^{-2});
- γ' = submerged soil unit weight ($ML^{-2}T^{-2}$);
- γ_f^p = plastic deviatotic shear strain at softening completion (–);
- Δ = upward pipe displacement, or mobilization distance (L);
- δ_f = upward pipe displacement, or mobilization distance, at peak uplift resistance (L);
- ξ = state parameter (–);
- μ = interface frictional coefficient between pipe and soil (–);
- υ_p = Poisson's ratio of pipe (-);
- τ = frictional shear stress ($ML^{-1}T^{-2}$);
- τ_{crit} = maximum allowable frictional shear stress ($ML^{-1}T^{-2}$);
- σ'_n = contact pressure between pipe and soil ($ML^{-1}T^{-2}$);
- ϕ_{crit} = critical state soil intergranular friction angle (–);
- ϕ_{max} = peak friction angle of soil (–);
- ϕ_μ = interface friction angle between pipe and soil (–);
- Ψ = angle of dilation for granular soils in shear (–);
- ψ_{max} = ultimate dilation angle of soil (–); and
- ψ_{res} = residual dilation angle of soil (–).

References

ABAQUS [Computer software]. Providence, RI.

American Society of Mechanical Engineers (ASME). (2012). "Gas transmission and distribution piping systems." *B31.8*, New York.

ASCE. (1984). "Guidelines for the seismic design of oil and gas pipeline systems." *Committee on Gas and Liquid Fuel Lifelines of the ASCE Technical Council on Lifeline Earthquake Engineering*, Reston, VA.

Been, K., and Jefferies, M. G. (1985). "A state parameter for sands." *Geotechnique*, 35(2), 99–112.

Bolton, M. D. (1986). "The strength and dilatancy of sands." *Geotechnique*, 36(1), 65–78.

British Standards Institution. (2004). "Code of practice for pipelines Steel pipelines on land." *PD8010-1*, London.

Cheong, T. P. (2006). "Numerical modelling of soil-pipeline interaction." Ph.D. thesis, Univ. of Cambridge, Cambridge, U.K.

Cheuk, C. Y., White, D. J., Bolton, M. D. (2008). "Uplift mechanisms of pipes buried in sand." *J. Geotech. Geoenviron. Eng.*, 10.1061/(ASCE)1090-0241(2008)134:2(154), 154–163.

Croll, J. G. A. (1997). "A simplified model of upheaval thermal buckling of subsea pipelines." *Thin-Walled Struct.*, 29(1–4), 59–78.

Dasari, G. R., and Soga, K. (2000). "A guide book for soil models and soil-pipe analysis using ABAQUS." *Rep. submitted to Tokyo Gas*, Tokyo, Japan.

Det Norske Veritas (DNV). (2007). "Global buckling of submarine pipelines—Structural design due to high temperature/high pressure." *RP-F110*, Oslo, Norway.

Dickin, E. A. (1994). "Uplift resistance of buried pipelines in sand." *Soils Found.*, 34(2), 41–48.

Dickin, E. A., and Laman, M. (2007). "Uplift response of strip anchors in cohesionless soil." *Adv. Eng. Software*, 38(8–9), 618–625.

Jefferies, M. G. (1993). "Nor-Sand: A simple critical state model for sand." *Geotechnique*, 43(1), 91–103.

Palmer, A. C., et al. (2003). "Uplift resistance of buried submarine pipelines: comparison between centrifuge modeling and full-scale tests." *Géotechnique*, 53(10), 877–883.

Palmer, A. C., Ellinas, C. P., Richards, D. M., and Guijt, J. (1990). "Design of submarine pipelines against upheaval buckling." *Proc., Offshore Technology Conf.*, OTC, Houston, TX, 551–560.

Pedersen, P. T., and Jensen, J. J. (1988). "Upheaval creep of buried pipelines with initial imperfections." *Marine Struct.*, 1(1), 11–22.

Robert, D. J. (2010). "Soil-pipeline interaction in unsaturated soils." Ph.D. thesis, Univ. of Cambridge, Cambridge, U.K.

Robert, D. J., and Soga, K. (2010). "Soil pipeline interaction in unsaturated soils." Chapter 13, *New trends in the mechanics of geomaterials*, Wiley, Lausanne, Switzerland.

Schaminée, P. E. L., Zorn, N. F., and Schotman, G. J. M. (1990). "Soil response for pipeline upheaval buckling analysis: Full-scale laboratory tests and modelling." *Offshore Technology Conf.*, OTC, Houston, TX.

Thusyanthan, N. I., Mesmar, S., Robert, D. J., Wang, J., and Haigh, S. K. (2011). "Upheaval buckling assessment based on pipeline features." *Offshore Technology Conf.*, OTC, Houston, TX.

Thusyanthan, N. I., Sultan, M., Wang, J., Haigh, S. K. (2010). *Uplift resistance of buried pipelines and DNV guidelines*, IBC Energy, London.

Trautmann, C. H., and O'Rourke, T. D. (1983). "Behaviour of pipe in dry sand under lateral and uplift loading." *Geotechnical Engineering Rep. 83-7*, Cornell Univ., Ithaca, NY.

Wang, J., Haigh, S., Forrest, G., and Thusyanthan, N. (2012). "Mobilization distance for upheaval buckling of shallowly buried pipelines." *J. Pipeline Syst. Eng. Pract.*, 10.1061/(ASCE)PS.1949-1204.0000099, 106–114.

White, D. J., Barefoot, A. J., Bolton, M. D. (2001). "Centrifuge modelling of upheaval buckling in sand." *Int. J. Phys. Modell. Geotech.*, 2(1), 19–28.

Williams, E. S., Byrne, B. W., and Blakeborough, A. (2013). "Pipe uplift in saturated sand: Rate and density effects." *J. Geotechnique*, 63(11), 946–956.

Yimsiri, S., Soga, K., Yoshizaki, K., Dasari, G. R., and O'Rourke, T. D. (2004). "Lateral and upward soil-pipeline interactions in sand for deep embedment conditions." *J. Geotech. Geoenviron. Eng.*, 10.1061/(ASCE)1090-0241(2004)130:8(830), 830–842.